Radiation Measurements 183 (2025) 107403

Contents lists available at ScienceDirect

Radiation Measurements

journal homepage: www.elsevier.com/locate/radmeas

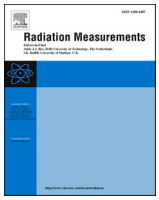

Calibration of $^{90}Sr + {}^{90}Y$ planar sources using thermoluminescent dosimeters, radiochromic film, a PMMA phantom and Monte Carlo simulation

Daniel Litvac *, Linda V.E. Caldas

Instituto de Pesquisas Energéticas e Nucleares / Comissão Nacional de Energia Nuclear (IPEN/CNEN-SP), Av. Prof. Lineu Prestes 2242, São Paulo, Brazil

ARTICLE INFO

Keywords:
Beta radiation
Dermatological applicators
Beta therapy
Dosimetry

ABSTRACT

In some parts of Brazil, $^{90}Sr + {}^{90}Y$ clinical applicators are still in use for dermatological and ophthalmic treatments, even with new technologies worldwide, because they are of lower cost and easier use. Calibration and periodic recalibration of these applicators to verify the absorbed dose rate is essential to ensure accuracy in clinical treatments. This work focused on an alternative calibration method for $^{90}Sr + {}^{90}Y$ sources, utilizing thermoluminescent dosimeters, radiochromic films, and Monte Carlo simulation, following international recommendations. Regarding radiation doses, the thermoluminescent response of μLiF pellets and the response of radiochromic films were evaluated to determine reproducibility, linearity of response, and their dose-response curves. Additionally, radiochromic films were used to determine the dose rate distribution across the areas of the clinical applicators, and the μLiF dosimeters were used as a comparative measure in determining the axial central dose rate of clinical applicators. A PMMA phantom was developed and utilized to perform the calibrations. Monte Carlo simulation was essential for replicating the radioactive properties and correction factors for radiation and deposited doses in two media and at different distances from these sources. This work presents a practical and cost-effective method for calibrating planar $^{90}Sr + {}^{90}Y$ radioactive sources; it was developed to serve locations that lack state-of-the-art technological resources, and was validated for effectiveness and broad applicability. The developed technique allows for long-distance calibration using dosimetric materials, provided they are properly handled and shielded.

1. Introduction

The demand for radiotherapy and brachytherapy in Brazil is unfulfilled. The lack of linear accelerators instigates the search for alternatives that may replace this kind of instrument. Brachytherapy is a form of radiation therapy where a radiation source is placed inside or next to the area requiring treatment.

Twelve percent (three of 26) of the Brazilian states do not have linear accelerators and 15% (four of 26) do not have brachytherapy centers. Beta therapy, a type of brachytherapy, is one of these alternatives that the Brazilian Unified Health System and private services still use to supply the demand (Rosa et al., 2023).

Beta $^{90}Sr + {}^{90}Y$ clinical applicators with a half-life of 28.8 years (Friedell et al., 1950) are still in use for dermatological and ophthalmic treatments in Brazil. Calibration and periodic recalibration of these applicators, to verify the absorbed dose rates, are essential procedures for quality assurance in clinical treatments (ISO, 2009).

Since 1977, the National Institute of Standards and Technology (NIST) has offered a standard calibration service. In 1989, following an international comparison of surface absorbed dose rates, NIST's calibration procedure was revised (Soares, 1991; Dias and Caldas, 1998), and the results of the first five years of NIST calibrations using the revised method were subsequently presented. Both NIST and Amersham have well-established calibration procedures, employing different techniques and slightly varying factors in dose-rate determinations for beta-ray applicators, as noted by Soares (1995). Although the results show a 13% difference, this may not be significant given the associated measurement uncertainties.

Many older applicators still in use were calibrated by manufacturers using outdated methods unsuitable for beta dosimetry (Soares, 1995).

This article is part of a special issue entitled: SSD20 Proceedings published in Radiation Measurements.

* Corresponding author.
E-mail addresses: daniel.litvac@usp.br (D. Litvac), lcaldas@ipen.br (L.V.E. Caldas).

https://doi.org/10.1016/j.radmeas.2025.107403
Received 28 February 2024; Received in revised form 9 February 2025; Accepted 14 February 2025
Available online 22 February 2025

In 2004, studies and techniques were published in the ICRU Report 72 (Cross et al., 2004), demonstrating further improvements that should be implemented to standardize and ensure better precision and efficiency in the calibration of these clinical applicators. In 2009, a standard was published in England that established and determined these updated methods and techniques, which are still in effect today (ISO, 2009).

Despite this evolution of documents and standards on the subject, many clinics and hospitals in Brazil use calibrations provided by the manufacturers of clinical applicators, often performed in the 20th century. To ensure better quality control, some facilities in Brazil seek calibration alternatives, such as using an extrapolation chamber as a secondary standard. In regions without access to such detectors, they turn to more affordable and feasible options like thermoluminescent dosimeters or radiochromic films.

The field of thermoluminescent dosimetry has expanded since the 1960s, with major publications involving appropriate materials for personal dosimetry. In the same decade, research focused on the thermoluminescence of lithium fluoride (LiF). The high sensitivity and good response stability of this material have been proven, enabling applications within important areas of medicine (ISO, 2009).

In thermoluminescent analysis, the precision of detecting emitted light is crucial. Thermoluminescence is a process where a material emits light upon being heated, and the emitted light intensity is used to measure ionizing radiation exposure. The low dispersion property of LiF ensures that the light emitted by the sample remains focused and does not scatter extensively in the visible region. This significantly enhances the accuracy of the measurements by minimizing potential interferences caused by light dispersion. Its dosimetric applications are very well known and used in radioprotection and medicine procedures. LiF:Mg, Cu,P and LiF:Mg,Ti detectors are some of the most popular thermoluminescent dosimetrie (TLD) materials for personal, environmental and clinical dosimetry due to their high sensitivity and equivalence to human tissue (McKeever et al., 1995; Furetta, 2010; Horowitz, 2014).

The TL phenomenon is represented as a function of heating time or temperature. Heating is the necessary stimulus for light emission with energy proportional to that deposited by ionizing radiation (Furetta, 2008; Horowitz, 2014). If the materials are associated with a transducer, the emitted light signal is transformed into an electrical signal. In this way, it is possible, with the help of a photomultiplier tube, to measure, proportionally, the radiation dose that was initially deposited on the TL materials.

Since 1980, radiochromic films were developed and used for medical dosimetry too. Several publications and reviews demonstrate the importance of these applications, due to their property to record intensity of color changes in response to radiation exposure. They are valuable tools for measuring and verifying radiation doses in various applications such as radiotherapy and material testing, providing accurate and visual information that helps ensure the safety and efficacy of radiation-involved processes (Soares, 2006; Soares et al., 2009; Niroomand-Rad et al., 2020).

Some of these applications involve radiotherapeutic procedures in dermatological beta therapy, ophthalmological beta therapy and beta therapy for pterygium prophylaxies, which are formalized in the Brazilian Unified Health System (SUS Ministry of Health, 2022). These procedures are intended to prevent and treat the formation of keloids, small malignant neoplasms of the skin and cases of pterygium. $^{90}Sr + ^{90}Y$ is one of the possible sources used for this type of treatment. In NN 3.01, "Basic Radiological Protection Guidelines", updated in March 2014, it is specified in item 5.13.1.1 that holders of clinical services, private or public, should ensure the calibration of equipment and sources for clinical dosimetry, with supervision of experts qualified by the Brazilian Nuclear Energy Commission (CNEN National Commission on Nuclear Energy, 2014).

These clinical applicators are coated with specific materials, and their geometry affects how radioactive beams are emitted. These unique characteristics make it essential to study and use these sources with the assistance of radiation transport simulations (ISO, 2009).

The relative axial depth-dose data distribution in water for planar sources of $^{90}Sr+^{90}Y$ was determined by Soares et al. (2001), using different dosimetry methods. The data showed good agreement with Monte Carlo radiation transport simulation (Cross et al., 2001).

Geant4 is a Monte Carlo simulation toolkit; it has a radiation transport package for scientists, physicists and medical physicists, and it can be used to assist in the calibration of beta clinical applicators (Agostinelli et al., 2003; ISO, 2009). Some researchers around the world developed a software system for Geant4-based simulation called GAMOS. This software is a framework for simulations in different physics fields with a friendly user interface (Arce et al., 2014).

The best calibration methods for these sources are not always available in a certain country or continent, such as a primary standard laboratory. In these cases, alternative calibration methods are resorted to, which can meet the demand. The objective of this work was to establish a calibration method of beta therapy clinical applicators based on the guidelines of the international standard ISO 21439 (2009), providing a practical and more cost-effective way to perform calibrations, and help institutions and hospitals follow the standards and best practices related to the subject.

2. Materials and methods

This work was conducted at the Radiation Metrology Center of IPEN/CNEN/São Paulo, and its stages are described below.

2.1. Dosimetric samples

Fifteen samples of LiF: Mg, Ti (TLD-100 Microcube), Thermo Scientific™, cubic format with dimension of 1 mm, were dosimetrically characterized. In addition, the mass of these samples was measured to correct the obtained data.

Square strips (2.5 cm^2) of GAFChromic™ EBT3 Film were used from a A4 sheet (210 mm × 297 mm) of the radiochromic film to verify the $^{90}Sr + ^{90}Y$ source dose rates and dose distributions. The film contains an active layer (28 μm) sandwiched between 125 μm matte-surface polyester substrates and a dynamic dose range of 0.1–20 Gy (GAFChromic™, 2018).

2.2. Monte Carlo simulation

Based on the Cross et al. (2001) method, this work reproduced the relative axial depth-dose data distribution for planar sources in two different infinite media, water and polymethyl methacrylate (PMMA) using the Geant4 simulation toolkit and GAMOS framework. Correction factors based on absorbed dose in water and PMMA for different depths were determined. For the simulation, it was considered that the clinical applicator had a homogeneous distribution of $^{90}Sr + ^{90}Y$ in its area, and it was performed by replicating the setup of clinical applicators, with a resolution of 1 mm^3 voxels and 10^8 events, achieving less than 1% uncertainty for absorbed doses. Fig. 1 shows the energy spectrum used in the simulations.

2.3. Radiation systems

Two radiation systems were used to characterize the dosimetric materials. The first is part of a Risø reader system, Risø TL/OSL-DA-20 model, a $^{90}Sr + ^{90}Y$ source with a dose rate of 0.1 Gy/s, 2010, at 0.7 mm of distance in air. The second is a $^{90}Sr + ^{90}Y$ source from the beta secondary standard system (BSS2) with a dose rate of 123.32 μGy/s at a distance of 11 cm from the source, 2005, Amersham Buchler, calibrated in the German Primary Standard Laboratory, Physikalisch-Technische Bundesanstalt (with $k = 2$).

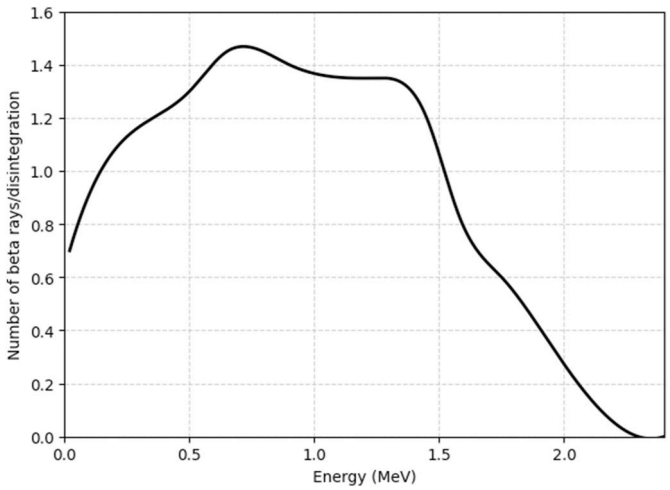

Fig. 1. Energy spectrum of $^{90}Sr + {}^{90}Y$ (ISO, 2009; Mostafa et al., 2016).

2.4. Reader systems

A TL reader system was used, Risø TL/OSL-DA-20, with a heating rate of 10 °C/s and constant N_2 flow of 5.01/min, reaching a temperature of 400 °C for the TL reading.

For the film readings, the EPSON Expression 11000XL was utilized. The scanner has the size of an A3 sheet with a maximum resolution of 12800 dpi and a color resolution of 48 dpi.

2.5. Annealing treatment for sample reuse

For TLD samples, after irradiation, it is crucial to remove any remaining trapped electrons to prepare the samples for accurate measurement of the accumulated radiation dose. The samples were subjected to heat treatment. A muffle furnace was used and the μLiF was treated at 400 °C for 1 h followed by 100 °C during 2 h (McKeever et al., 1995; Furetta, 2008).

2.6. Clinical beta therapy applicator calibration

The Calibration Laboratory of the Radiation Metrology Center at IPEN has two dermatological plane surface source applicators with manufacturer calibration certificates. The calibration procedure for these two clinical applicators was realized using the TLD materials and radiochromic films based on the recommendations described by the international standard (ISO, 2009). Table 1 shows the characteristics of the clinical applicators. The physical dimension is the active area.

Key documents involving brachytherapy sources state that a clinical applicator calibration should be in accordance with the dose rate in water. Dosimeters should be calibrated against a primary or secondary standard radioactive material to ensure accurate and consistent measurements in Brachytherapy applications (ISO, 2009).

Primary standards are directly traceable to internationally recognized reference materials and are used as the ultimate reference for calibration. Secondary standards, on the other hand, are derived from primary standards and are used for routine calibration purposes in laboratories and facilities where direct access to primary standards may be limited.

The calibration of clinical applicators must be performed at a distance of 1 mm in water with the detector positioned at the central axis of the radioactive area. By using radiochromic films, it is possible to divide the total area of the planar source into pieces of 1 mm^2 and, for each piece, determine the dose rate at this positioning and standard distance. The central area pieces are the main ones to be determined and used as a dose reference; and it is recommended to use detector sizes of maximum 1 mm^2 (Cross et al., 2004; ISO, 2009; ISO, 2023).

Table 1
Features of dermatological clinical applicators.

Source	Model	Dimension Active area (cm^2)	Manufacturer calibration dose rate in tissue surface (Gy/s)	Calibration date
Square	*Amersham/ SIQ18*	2.0 x 2.0	0.056	Nov 08, 1968
Rectangular	*Amersham/ SIQ21*	2.0 x 1.5	0.053	Sep 17, 1986

2.7. Uncertainties

The combined uncertainty is shown in Equation (1). The analysis was performed considering the type An uncertainties, statistical uncertainties related to measurements, and type B uncertainties that are related to equipment performance. This work maintained a 95% confidence level as expected by the standard.

$$\sigma_{total}^2 = \sigma_A{}^2 + \sigma_B{}^2 \quad (1)$$

where σ_A is type An uncertainties, σ_B is type B uncertainties and σ_{total} is total uncertainties.

Type B uncertainties are the uncertainty of the BSS2, those associated with the Risø TL/OSL-DA-20 and the EPSON Expression 11000XL readers.

- Uncertainty of the Risø TL/OSL-DA20 Reader for TL measurements: ±0.05%
- Uncertainty of the EPSON Expression 11000XL Reader for TL measurements: ±0.3%
- Uncertainty in the thermal treatment temperature: ±0.04%
- Uncertainty of the BSS2 radiation systems: ±2% ($k = 2$)

Type An uncertainties are those associated with the values obtained from the irradiated dosimetric materials, where the calculation of equation (1) is implicitly included.

Furthermore, the uncertainty analyses consisted of the use of error propagation shown in Equation (2) (Bevington and Robinson, 2003; BIPM, IEC, IFCC, ILAC, ISO, IUPAC, IUPAP, OIML, 2008):

$$\sigma_u{}^2 = \sum_{i=j}^{N} (\partial u / a_i)(\partial u / a_j)(cov(a_i a_j)) \quad (2)$$

where σ_u is the uncertainty of u, $\partial u/a_i$ is the partial derivative of u with respect to a_i, $\partial u/a_j$ is the partial derivative of u with respect to a_j and cov (a_i,a_j) is the covariance between a_i and a_j.

2.8. Dosimeter characterization

The samples, TLDs and radiochromic films, were characterized according to the following tests. For all tests, several measurements were performed.

For the two types of dosimetric materials, the reproducibility test was conducted to evaluate the consistency of the dosimeter responses. Dosimeter response for a specific dose should not exceed an uncertainty margin of 5% ($k = 1$) over consecutive readouts, as per the guidelines established by Furetta (2008). The requirement of a 5% uncertainty margin is critical as it ensures the precision and reliability of the dosimetric measurements, reflecting the dosimeter ability to produce consistent readings under identical conditions. The reason for this limit is related to the need to minimize variations that could distort the final results and compromise the validity of the conclusions. In TL studies, small errors can lead to significant deviations in dating or radiation dose

measurements. A reproducibility error greater than 5% could significantly undermine the interpretation of the data.

Only for the TLD materials, the sensitivity test was conducted for each sample to determine the response distribution of the sample population, subsequently selecting samples with better reproducibility and falling within the same sensitivity value group (Furetta, 2008).

Equation (3) shows the TL measurement for the individual sample, where M_{raw} is the set reading and M_{bgk} is the background reading. Eliminating background radiation is crucial due to grid fluctuations and equipment reading fluctuations.

Equation (4) shows the sensitivity obtained for each sample, where M_{corr} is the TL measurement for the individual sample, D is the absorbed dose, m is detector mass and f ' is the sensitivity of the sample:

$$M_{corr} = M_{raw} - M_{bkg} \tag{3}$$

$$f' = M_{corr}/D.m \tag{4}$$

Using the secondary standard source BSS2, the samples, TLD or radiochromic film, were irradiated within a dose range as shown in Fig. 2. For each dose, five repeated cycles were performed to determine the uncertainties.

The linearity of the dose-response curves was verified using the Marquardt method and the Coefficient of Determination (R^2) was obtained too. Uncertainties were determined by error propagation for dependent and independent variables applied when necessary for each case (Bevington and Robinson, 2003; BIPM, IEC, IFCC, ILAC, ISO, IUPAC, IUPAP, OIML, 2008).

2.9. Dose calculation of a ^{90}Sr+^{90}Y dermatological applicator

$D_{PMMA:1mm}$ is the dose determined by the interpolation equation obtained through the linearity test and shown in Equation (5). Linearity and dose-response curves were established between 0.2 Gy and 0.7 Gy using the secondary standard BSS2 system with a ^{90}Sr + ^{90}Y radioactive source.

The constants a and b are from the straight line function, angular coefficient and linear coefficient, respectively.

For each TLD and for radiochromic film, Equation (6) describes the dose calculation at 1 mm depth in water, and it is analogue to the equation described at AAPM TG 191 (Kry et al., 2020). The equation is analogous because it follows the guidelines where, for a radioactive source, dosimetric calibration should be based on the medium material and its depth, necessitating the establishment of correction factors when using phantoms and methods that can be numerically corrected when necessary.

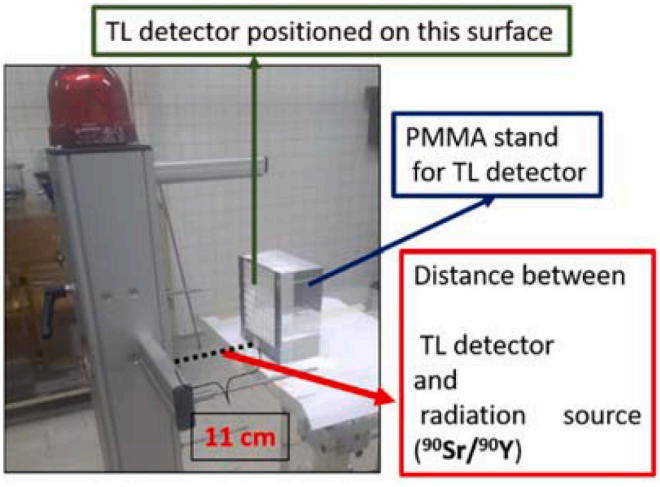

Fig. 2. Sketch describing the irradiation position for TL detector calibration using the BSS2 system.

Relative depth doses in water from the ^{90}Sr+^{90}Y planar sources have been calculated by Geant4 (GAMOS-6.1.0.) code and the results were compared to the reference data (Soares et al., 2001; Cross et al., 2001, 2004).

For the simulation, the radioactive material was inserted into a disk (negligible thickness), with a diameter of 1 cm, or on a rectangular surface. In both cases, it was covered by a 0.1 mm thick stainless-steel window. The variation in the dimensions (rectangular or disk) of the radioactive surface does not interfere in the results obtained regarding the dose rates at depths in the simulated media, tested for both scenarios and obtaining the same result. All simulations were conducted based on determinations from ISO standard (ISO, 2009), procedures and criteria set forth by the ISO standard to ensure consistency, accuracy, and reproducibility of the results.

The material of a detector with a volume up to 1 mm^3 is not relevant in the simulation, as confirmed by the values obtained by Cross et al. (2001). Changing the material that has a volume of 1 mm^3 is not relevant to the simulation configuration because the correction factors will remain the same for the different depths of the medium in which this material is immersed. This finding aligns with theoretical principles that suggest small detector volumes minimize perturbation effects, thereby ensuring accurate dose measurements (ISO, 2009). Additionally, the uncertainties associated with the absorbed dose in water and PMMA are maintained below 1%, highlighting the high precision and reliability of the simulation results. Such low uncertainty levels are crucial for dosimetric accuracy, ensuring that the absorbed dose measurements closely reflect the actual dose delivered, which is essential for both clinical and research applications in radiation dosimetry. These simulation results are presented in Table 2, and both circular and rectangular applicators showed this result.

The radioactive material was mounted in an infinite water or PMMA media. Through this simulation, the dose correction factors $N_{PMMA,w}$. and $N_{w:1.8mm,w:1mm}$ were obtained.

$$D_{PMMA:1mm} = a.M_{corr} - b \tag{5}$$

$$D_{w:1mm} = D_{PMMA:1mm}.N_{PMMA,w}.N_{w:1.8mm,w:1mm}.k_{\theta}.k_f \tag{6}$$

$N_{PMMA,w}$ is the dose-to-water correction factor. For beta applicator calibration, a Polymethyl methacrylate (PMMA) phantom was developed to reproduce an environment where the source surface is located at 1 mm from the dosimeter sample at the axis center geometry, using the depth-dose data equivalence between PMMA and water to determine the dose in water (Cross et al., 2004; ISO, 2009; ISO, 2023).

$N_{w:1.8mm,w:1mm}$ is the dose correction factor for dose from 1.18 mm depth in water to 1 mm depth in water. When determining the dose from the applicator at a depth of 1.18 mm in water, it is necessary to apply a correction factor based on the environment of these applicators to adjust the dose to a depth of 1 mm. The scenarios were simulated obtaining absorbed dose values for both depths with uncertainties less than 1%.

During the reproducibility tests, all samples were irradiated in three different angles of radiation beam incidence of the BSS2. The angular dependence was determined to 15°, 30° and a maximum of 45°, considering the source-detector distance and the maximum dimensions of the radioactive plates. For reference angulation (0°), the flat surface

Table 2
Relative measured axial depth-dose distributions in water for a planar ^{90}Sr +^{90}Y source at a 1 mm^3 volume.

Depth in water (mm)	Relative measured axial depth	Uncertainty (%)
0.00	1.752	0.30
0.50	1.349	0.30
1.00	1.000	0.30
1.18	0.903	0.30
1.50	0.752	0.30

of the dosimeters was placed perpendicular to the radiation beam. This method was used to validate the reproducibility, once the non-interference of the angular position of the detector with radiation incidence was confirmed. The calculation uncertainties of reproducibility remained the same when changing the angle, demonstrating no need to use this correction factor in the calculations. The k_θ value was equal to 1.

For fading correction (k_f), all measurements were taken irradiating every detector, and waiting 24h and 120h for the TL readings. This procedure was undertaken to compare and guarantee 2% of fading after one day and keep the TL signal for five days within the values accepted in the reproducibility test. According to McKeever et al. (1995) and Furetta (2010), the decay of the μLIF TL signal occurs 24 h after irradiation, equivalent to 2% of the total signal, and remains stable for three months. Therefore, for all measurements, the k_f value was equal to 1.

After determining all correction factors and with dosimeters having well-defined dose-response curves, it was possible to use the phantom to calibrate clinical applicators using the dosimeters.

3. Results

For the experimental setup described, dose correction factors were determined for different depths in water. The ratio between the dose at a certain depth and the dose at another depth determines the different correction factors. Since the dose uncertainty is less than 1%, the uncertainties of the correction factors become less than 1% when performing error propagation, as shown in Table 2.

The relative measured axial depth-dose distributions in PMMA to water for a planar $^{90}Sr + {}^{90}Y$ source at a 1 mm^3 volume is (0.99 ± 0.30%) and (1.107 ± 0.32%) for 1 mm depth in PMMA to 1.18 mm depth in water.

The values obtained in Table 2 correspond to the reference values (Soares et al., 2001; Cross et al., 2004; ISO, 2009) and have uncertainties below 1%. Thus, it was possible to use the simulation configurations for the applications in water and PMMA in this work.

For the selection of TLD samples, five cycles of irradiation and measurements were conducted for 0.6 Gy dose, and the mean value, the standard deviation (SD) and the standard deviation of the mean value (SDM) were calculated.

For all measurements, the background radiation values were initially determined. The measurements were normalized to the values obtained without irradiation of each sample (for non-irradiated samples).

The sensitivity histogram in Fig. 3 shows the best samples for detection at lower absorbed doses and groups of samples with the same result.

Five TLD pellets with excellent reproducibility, uncertainty value below 5%, were chosen to generate the dose-response curve using the BSS2 standard. Table 3 displays the statistical uncertainties in reproducibility of the TL response, determining the standard deviation (SD), relative standard deviation (RSD) and percentual relative standard deviation (PRSD).

Table 3
TL measurements and related uncertainties for five measurement cycles of μLiF samples, irradiated with 0.5 Gy of beta radiation, Risø system. Standard deviation (SD), relative standard deviation (RSD) and percentual relative standard deviation (PRSD).

Sample	Mean (a.u.)	SD (a.u.)	RSD (a.u.)	PRSD (%)
1	48241	1906	852	1.8
2	54433	2009	898	1.6
3	40723	1766	790	1.9
4	56048	1259	563	1.0
5	40105	1331	595	1.5

Fig. 4 shows the TL emission curve of a μLiF sample.

The μLiF TL curves exhibit the main peak at around 160 °C, and these curves represent signals collected 24 h after irradiation. The values obtained from these measurements fall within the recommended range for uncertainties (ISO, 2009).

For radiochromic films, 1 cm^2 slices were cut for the tests. The Python programming language was used to process scanned images of the irradiated films. It allows the transformation of images into numerical matrices based on pixels and their respective color intensities that compose them, determining the standard deviation (SD), relative standard deviation (RSD) and percentual relative standard deviation (PRSD) for red color intensity.

The radiation dose is based on the intensity of the red color in each pixel of the image generated from the radiochromic film. The reproducibility of the radiochromic films was determined, and Table 4 presents their associated uncertainties.

Linearity and dose-response curves were established between 0.2, 0.3, 0.4, 0.5, 0.6 and 0.7 Gy using the secondary standard BSS2 system with a $^{90}Sr + {}^{90}Y$ radioactive source.

The dose-response curves were determined for three μLiF samples and for the radiochromic sheet as a whole, based on square samples. A single curve was not determined for all μLiF detectors due to the high uncertainty that this procedure would cause, as individual curves have lower uncertainty, ensuring measurements within an acceptable range, established by the ISO standard (ISO, 2009).

The curves were obtained for five μLiF samples and are shown in Fig. 5. The linear correlation coefficients for each sample were around 0.988.

For the film, the dose-response curve also showed an acceptable metric, with a linear correlation coefficient equal to 0.998. The dose-response curve is presented in Fig. 6.

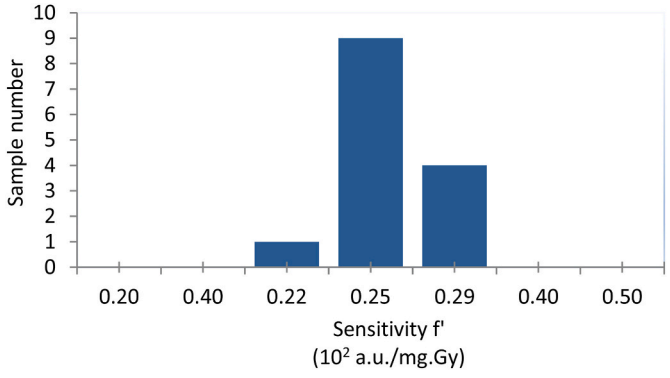

Fig. 3. Sensitivity histogram of μLiF samples, irradiated with 0.6 Gy of beta radiation, Risø system. TL reader system: Risø TL/OSL-DA-20.

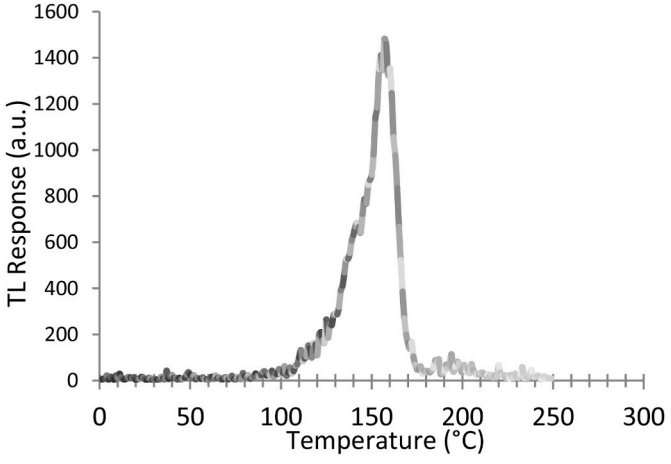

Fig. 4. TL emission curve of a μLiF sample, irradiated with 1 Gy of beta radiation, Risø system; TL reader system: Risø TL/OSL-DA-20.

Table 4
Measurements performed with radiochromic films and related uncertainties for five measurement cycles of GAFChromic™ EBT3 Film, irradiated with 0.5 Gy of beta radiation, Risø system. Standard deviation (SD), relative standard deviation (RSD) and percentual relative standard deviation (PRSD).

Red color intensity Mean Value (u.a.)	DS (a.u.)	RSD (a.u.)	PRSD (%)
89.8	1.0000	0.5771	0.01

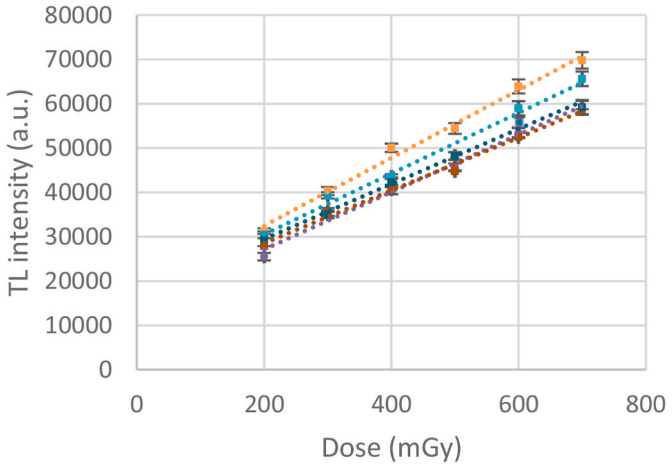

Fig. 5. Dose-response curves of five primary LiF samples used in the calibrations of beta radioactive sources.

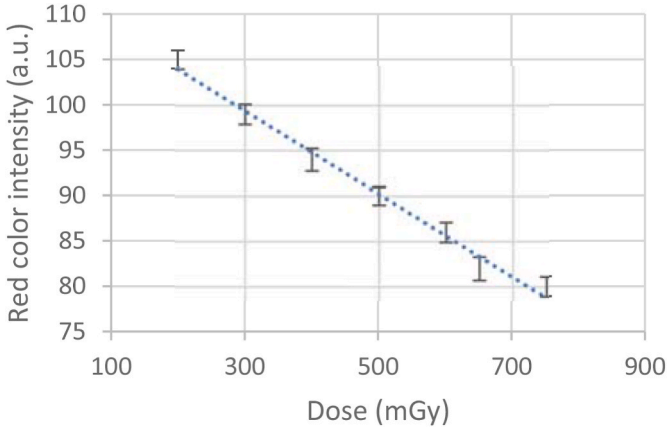

Fig. 6. Dose-response curve used in the calibrations of beta radioactive sources using radiochromic films.

With the curve adjustments obtained, it was possible to determine the values of Equation (5) for each dosimetric sample.

A PMMA phantom was developed for the calibration of clinical $^{90}Sr+^{90}Y$ applicators. In this setup, the surface of the radioactive source remains at 1 mm from a thermoluminescent dosimeter or a square radiochromic film sample positioned along the central axis of the applicator. Fig. 7 shows an image of this phantom. The development of this phantom was based on the standard (ISO, 2023). This standard defines the necessary dimensions to fully absorb beta radiation up to 5 cm depth of PMMA and ensures complete absorption within its dimensions while accounting for backscattering, maintaining the system as a simulation of a single material without air interference.

Another important aspect followed was the construction of the phantom in such a way that the fit of the dosimeters remained with less than 0.5 mm of space between air and PMMA. This spacing, as defined by the standard, results in negligible uncertainty between the phantom and the dosimeter. The phantom was custom-made, ensuring the upper and lower parts of the phantom fit precisely, leaving the dosimeter at a distance of 1 mm from the surface of any clinical applicator positioned.

The calibration of the two dermatological applicators, Amersham/SIQ18 and Amersham/SIQ21, was carried out using the developed phantom, and it was performed for both types of dosimetric materials, μLiF and radiochromic film.

Fig. 8 shows a scheme of the method developed and all steps.

The time chosen to irradiate the material is based on the dose rate provided by the clinical applicator manufacturer and the interval obtained from the dose-response curve of the dosimeters. Thus, for the two applicators calibrated in this study, the irradiation times for calibration were based on the values in Tables 5 and 6, establishing a standard irradiation time of 40 s. Repetition of five irradiations of the clinical applicator for calibration.

The calibration is performed manually by fitting the clinical applicator into the phantom. The time uncertainty due to handling during the fitting and removal of the applicator results in an uncertainty of 1% of the irradiation time.

The manual handling of the applicator replicates how treatment is carried out on patients. Using an automated system to open and close the radiation source would go against the purpose of this study, which aims to reduce costs while meeting the needs of care in countries with fewer resources.

3.1. Calibration of the square dermatological applicator Amersham/SIQ18

Table 5 shows the calibration values for applicator Amersham/SIQ18 using equations (5) and (6), with the two types of dosimetric materials, their respective uncertainties, and the percentage uncertainty variation between the manufacturer calibration and that of the respective material.

3.2. Calibration of the rectangular dermatological applicator Amersham/SIQ21

Table 6 shows the calibration values for applicator Amersham/SIQ21, with the two types of dosimetric materials, their respective expanded uncertainties ($\sigma_{expanded}$), and the percentage uncertainty variation (Δ) between the manufacturer's calibration and that of the respective material.

It can be observed that both calibrations (via TL and radiochromic film) resulted in a value lower than that presented by the manufacturer for the two radioactive sources. This outcome was expected due to the difference in the medium and the depth used by the manufacturer for calibration.

The comparison between the calibration values from the manufacturer and those from this work is necessary due to the requirements of the ISO standard (2009). Despite being different media and depths, this comparison is necessary to expose the level of uncertainty of the manufacturer versus that of this work. The standard states that a calibration performed at 0 mm depth is inadequate, causing high uncertainty as seen in manufacturer calibrations.

Comparing the two calibration methods, it can be concluded that the radiochromic film is more recommended, as its measurement uncertainty is lower, and it offers smaller dimensions of sensitive volume. This does not imply that μLiF cannot be used; they can be employed when they are the only option, with the reminder that the TL uncertainties should be an important point of consideration.

3.3. Determination of the dose distribution of the clinical applicators using radiochromic films

Using radiochromic films and the PMMA phantom, the dose distribution of dermatological applicators was determined. The area of each

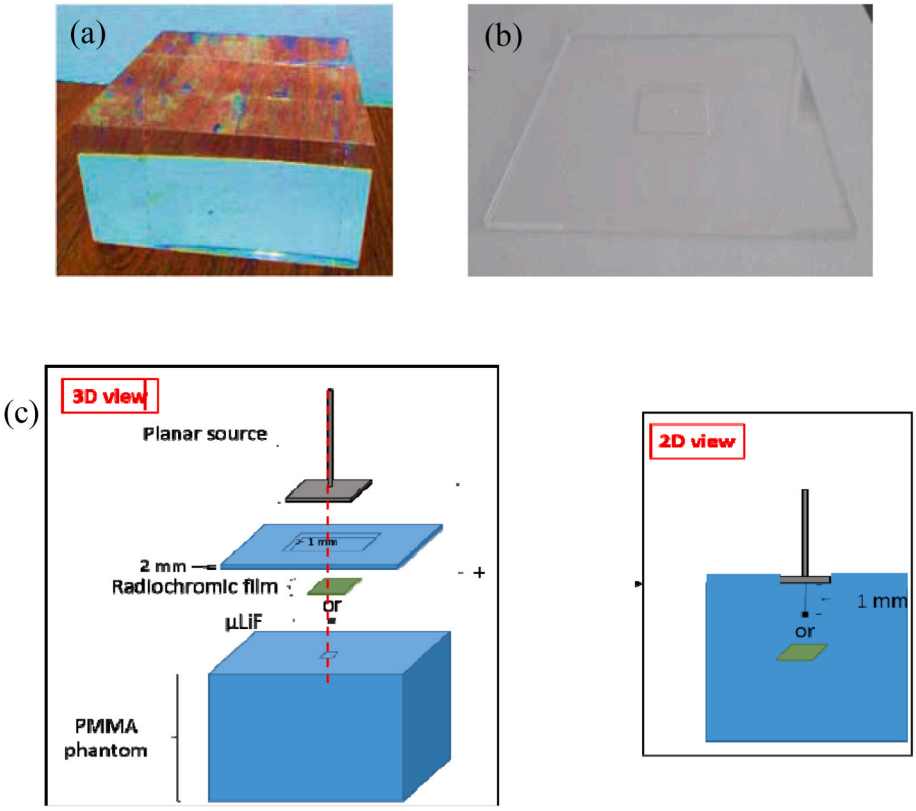

Fig. 7. PMMA simulator with dimensions of 50 x 100 × 100 mm^3, consisting of two attachable parts. The upper surface of (a) contains a recess for a thermoluminescent sample or a radiochromic film, and the surface of (b) contains a recess for fitting the clinical beta therapy applicator, (c) scheme of use and composition of the phantom for calibration of dermatological radioactive sources.

applicator was divided into 1 mm^2 squares, and for each square, a dose value was assigned. The squares on the central axis of the applicators served as a reference for normalizing the other values around them. Fig. 9 shows the distribution of doses from the planar radioactive sources.

The trend is for the central dose distribution (red values in Fig. 9) to be greater than the peripheral regions of the dermatological applicators. The normalization of dose points was based on the central area in relation to the main axis of the applicators; that does not imply that the maximum dose is always at the center; this is not the case due to the aging of the material. A hypothesis for this phenomenon is the uneven wear of the metallic coating on the applicator's emitting surface, a consequence of prolonged usage over the years.

4. Conclusion

This study introduces a practical and cost-effective technique for calibrating planar $^{90}Sr + {}^{90}Y$ radioactive sources. The effectiveness and broad applicability of the developed method were validated. Additionally, the dosimetric materials used can be transported over long distances if kept at room temperature, protected from light, and shielded from mechanical shocks. The developed method could be utilized for long-distance calibration while rigorously adhering to all aspects described in the study. However, there are some important considerations.

The uncertainty in the dose rate value determined through recalibration is acceptable when compared to the uncertainty provided by the manufacturer's calibration, which is used in the country. The percentage difference among the values is also acceptable, as the detection volume used by the manufacturer is greater than 1 mm^3, and the manufacturer calibration was performed on the surface skin rather than at 1 mm in water as in this work, following the ISO international standard. Radiochromic film results demonstrated a better response, with the measurement uncertainties remaining close to 5% ($k = 2$), as recommended by the standard.

The primary method for calibrating these radioactive sources is through extrapolation ionization chambers. However, when properly calibrated chambers are not available, the results of this work demonstrate that these methods serve as viable alternatives for calibration.

The old manufacturers, such as those of the applicators analyzed in this study and several others used in Brazil, performed calibration using extrapolation chambers with sensitive volumes larger than 1 mm^3, proving to decrease measurement precision and accuracy, thereby increasing uncertainties, rendering the method obsolete. With recent advancements, extrapolation chambers now have sensitive volumes as small as 1 mm^3, and calibrations are conducted at a depth of 1 mm to further enhance precision. The method presented in this study is modern, and it corrects these outdated and erroneous techniques used in the past. It represents continuous evolution, with well-structured techniques and creativity. It is a viable alternative for a calibration that refers to an old and outdated manufacturing process.

The main objective of this work has been achieved. People from other regions around the world, who may not have access to the best calibration alternatives but still use clinical applicators for dermatological patient treatment, can take inspiration and develop something similar or close to what was proposed in this work.

CRediT authorship contribution statement

Daniel Litvac: Writing – original draft, Visualization, Software, Methodology, Investigation, Formal analysis, Conceptualization. **Linda V.E. Caldas:** Writing – review & editing, Visualization, Validation, Supervision, Resources, Investigation, Funding acquisition, Conceptualization.

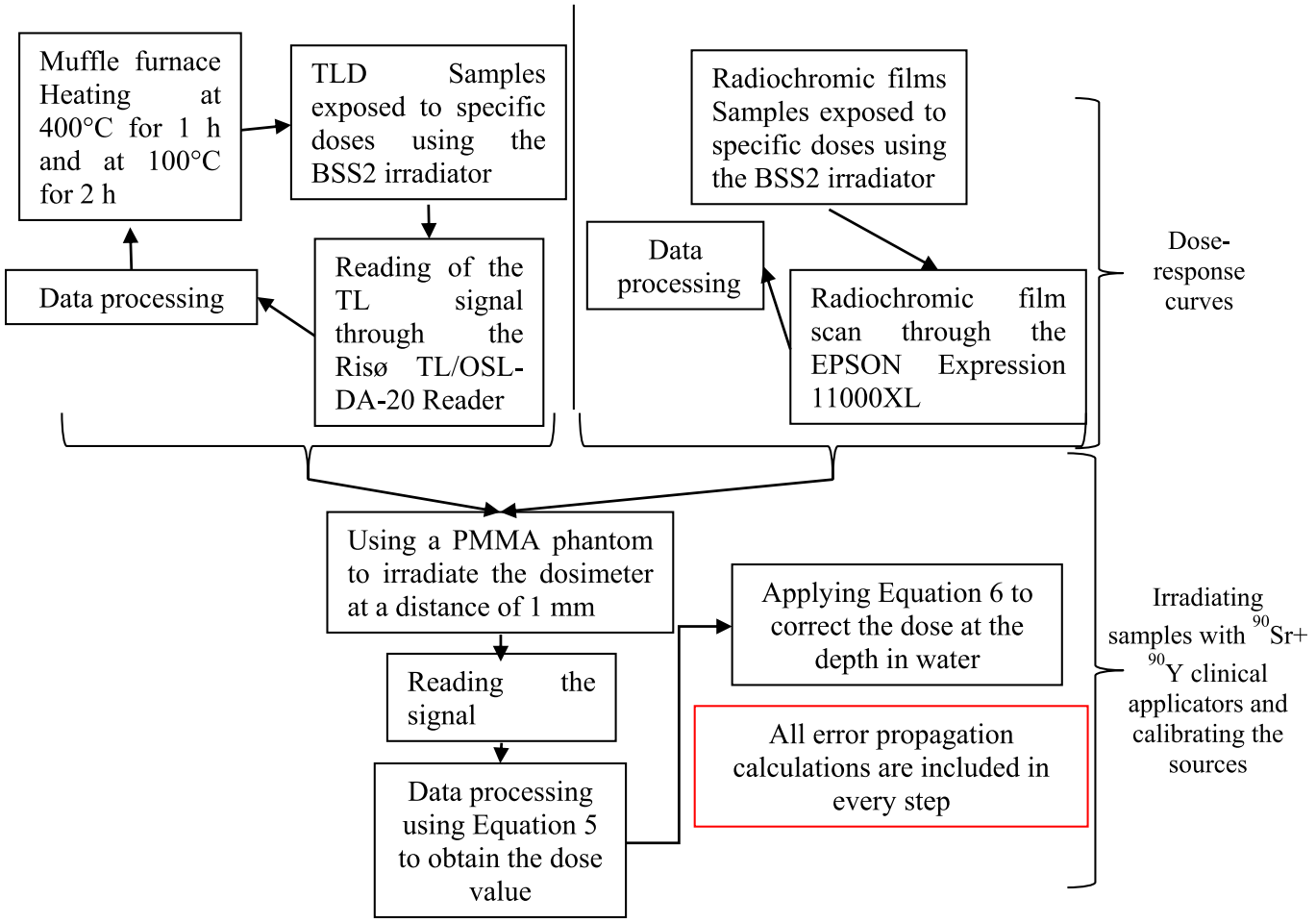

Fig. 8. An outline of the method used in this work to calibrate $^{90}Sr+^{90}Y$ clinical applicators.

Table 5
Calibration of the square dermatological applicator Amersham/SIQ18 for September 2023 reference date and comparison with the manufacturer's calibration and their respective calibration uncertainties. $\sigma_{expanded}$ is the expanded uncertainty and delta is the percentage difference between the manufacturer's calibration uncertainty and that of the respective material.

Calibration	σ_{reader} Type B (%)	σ_{BSS2} Type B (%)	σ_{time} Type A (%)	σ_a Type A (%)	σ_b Type A (%)	$\sigma_{N_{PMMA,w}}$ Type A (%)	$\sigma_{N_{w,1.8mm,w,1mm}}$ Type A (%)	Dose rate (Gy/s)	$\sigma_{expanded}$ k = 2 (%)	Δ (%)
Manufacturer (in skin surface)	–	–	–	–	–	–	–	0.014 ± 20%	–	–
μLiF (at 1 mm in water)	0.05	2.0	1.0	3.8	10.1	0.30	0.32	0.0099 ± 0.0013	13.6	32
Radiochromic Film (at 1 mm in water)	0.30	2.0	1.0	0.9	0.8	0.30	0.32	0.0097 ±0.0007	8.2	59

Table 6
Calibration of the rectangular dermatological applicator Amersham/SIQ21 for September 2023 reference date and comparison with the manufacturer's calibration and their respective calibration uncertainties. $\sigma_{expanded}$ is the expanded uncertainty and delta is the percentage difference between the manufacturer's calibration uncertainty and that of the respective material.

Calibration	σ_{reader} Type B (%)	σ_{BSS2} Type B (%)	σ_{time} Type A (%)	σ_a Type A (%)	σ_b Type A (%)	$\sigma_{N_{PMMA,w}}$ Type A (%)	$\sigma_{N_{w,1.8mm,w,1mm}}$ Type A (%)	Dose rate (Gy/s)	$\sigma_{expanded}$ k = 2 (%)	Δ (%)
Manufacturer (in skin surface)	–	–	–	–	–	–	–	0.022 ± 20%	–	–
μLiF (at 1 mm in water)	0.05	2.0	1.0	3.8	10.1	0.30	0.32	0.0200 ± 0.0020	10.3	48
Radiochromic Film (at 1 mm in water)	0.30	2.0	1.0	0.9	0.8	0.30	0.32	0.0172 ± 0.0008	5.1	74

(a)

	0	1	2	3	4	5	6	7	8	9	10	11	12	13	14	15	16	17	18	19	20	21
0	0.87	0.90	0.92	0.94	0.95	0.95	0.97	0.98	1.00	0.97	0.98	1.01	1.00	1.00	1.02	1.01	1.01	0.97	0.98	0.97	0.96	0.94
1	0.90	0.93	0.94	0.97	0.98	0.97	1.00	1.01	1.03	1.02	1.03	1.05	1.04	1.05	1.05	1.06	1.05	1.03	1.02	1.03	1.02	0.99
2	0.88	0.93	0.96	0.98	1.00	0.99	1.02	1.02	1.05	1.02	1.03	1.05	1.05	1.05	1.08	1.07	1.08	1.04	1.04	1.04	1.03	1.00
3	0.89	0.93	0.97	0.96	1.00	0.99	1.02	1.02	1.05	1.02	1.03	1.05	1.05	1.07	1.07	1.08	1.09	1.05	1.06	1.06	1.05	1.01
4	0.91	0.94	0.97	0.98	1.01	1.01	1.02	1.03	1.05	1.02	1.03	1.06	1.05	1.06	1.08	1.08	1.09	1.04	1.05	1.05	1.06	1.03
5	0.91	0.94	0.96	0.97	1.00	1.00	1.02	1.02	1.04	1.02	1.02	1.06	1.05	1.05	1.07	1.07	1.08	1.03	1.04	1.05	1.04	1.02
6	0.92	0.95	0.97	0.98	0.99	0.98	1.00	1.02	1.04	1.01	1.02	1.04	1.03	1.05	1.06	1.06	1.07	1.04	1.04	1.05	1.04	1.01
7	0.92	0.94	0.96	0.96	0.99	0.98	0.99	1.00	1.02	1.00	1.01	1.03	1.03	1.04	1.05	1.05	1.07	1.04	1.03	1.03	1.03	1.01
8	0.92	0.94	0.96	0.96	0.97	0.97	0.99	1.00	1.01	1.00	1.00	1.03	1.02	1.04	1.04	1.06	1.06	1.02	1.02	1.03	1.02	0.99
9	0.92	0.94	0.95	0.96	0.98	0.98	1.00	1.00	1.01	0.99	1.00	1.02	1.01	1.02	1.04	1.04	1.06	1.02	1.01	1.00	1.01	1.00
10	0.92	0.93	0.96	0.96	0.98	0.97	0.99	1.01	1.04	0.98	**1.00**	**1.00**	0.99	1.03	1.04	1.03	1.06	1.02	1.01	1.01	1.01	0.98
11	0.92	0.95	0.96	0.96	0.98	0.98	0.99	1.02	1.03	0.99	**1.00**	**1.00**	1.01	1.02	1.02	1.03	1.05	1.01	1.01	1.02	1.00	0.97
12	0.92	0.93	0.93	0.95	0.97	0.97	0.99	1.00	1.02	0.98	0.98	1.00	1.00	1.03	1.04	1.04	1.04	1.01	1.01	1.02	1.01	0.97
13	0.92	0.94	0.94	0.94	0.96	0.96	0.98	0.97	0.99	0.98	0.98	0.99	0.99	1.01	1.02	1.04	1.03	1.00	1.00	1.02	1.00	0.96
14	0.92	0.94	0.94	0.95	0.96	0.96	0.98	0.98	0.98	0.97	0.98	0.99	1.00	1.01	1.03	1.03	1.04	0.99	1.00	1.01	1.00	0.96
15	0.91	0.93	0.94	0.95	1.88	1.06	0.97	0.97	0.98	0.96	0.97	0.99	0.98	1.01	1.03	1.03	1.04	1.00	1.00	1.00	1.01	0.98
16	0.92	0.93	0.94	0.95	1.58	0.97	0.96	0.96	0.97	0.95	0.96	0.99	0.98	1.01	1.02	1.02	1.02	0.98	1.00	0.99	1.00	0.98
17	0.91	0.92	0.92	0.94	1.54	0.93	0.94	0.96	0.96	0.95	0.96	0.99	0.98	1.00	1.00	1.02	1.02	0.98	0.99	1.01	1.00	0.97
18	0.89	0.90	0.92	0.94	1.17	0.94	0.94	0.95	0.96	0.94	0.95	0.98	0.98	1.00	1.02	1.02	1.01	0.99	1.00	1.00	1.00	0.97
19	0.88	0.89	0.89	0.90	0.92	0.91	0.93	0.94	0.96	0.94	0.94	0.97	0.96	0.98	1.00	1.00	1.01	0.98	0.99	0.98	0.97	0.95
20	0.86	0.86	0.88	0.88	0.90	0.89	0.91	0.92	0.93	0.92	0.93	0.95	0.96	0.98	0.99	0.99	0.98	0.95	0.96	0.96	0.95	0.94
21	0.84	0.86	0.85	0.87	0.89	0.88	0.91	0.90	0.93	0.90	0.92	0.96	0.93	0.98	0.95	0.97	0.96	0.94	0.94	0.94	0.94	0.93

(b)

	0	1	2	3	4	5	6	7	8	9	10	11	12	13	14	15	16	17	18	19
0	0.70	0.71	0.74	0.76	0.76	0.75	0.74	0.73	0.71	0.70	0.69	0.68	0.68	0.68	0.68	0.67	0.66	0.66	0.65	0.64
1	0.68	0.71	0.75	0.78	0.79	0.79	0.77	0.75	0.73	0.71	0.70	0.69	0.68	0.68	0.66	0.66	0.65	0.64	0.62	0.61
2	0.68	0.74	0.80	0.86	0.88	0.87	0.85	0.83	0.81	0.78	0.76	0.74	0.72	0.71	0.70	0.69	0.67	0.65	0.63	0.61
3	0.69	0.76	0.86	0.92	0.96	0.95	0.94	0.92	0.90	0.89	0.86	0.84	0.82	0.79	0.77	0.74	0.72	0.67	0.64	0.61
4	0.69	0.77	0.88	0.95	0.99	0.98	0.97	0.96	0.96	0.96	0.95	0.94	0.92	0.88	0.87	0.83	0.78	0.72	0.66	0.61
5	0.69	0.78	0.89	0.95	0.99	0.99	0.98	0.98	0.98	0.98	0.98	0.97	0.96	0.95	0.93	0.90	0.86	0.76	0.67	0.62
6	0.69	0.79	0.90	0.97	0.99	1.00	0.99	0.99	1.00	1.00	0.99	0.97	0.98	0.97	0.96	0.94	0.89	0.79	0.68	0.61
7	0.70	0.80	0.91	0.97	0.99	1.01	1.00	0.99	1.00	0.99	1.00	0.99	1.00	0.98	0.98	0.96	0.91	0.80	0.68	0.61
8	0.70	0.80	0.92	0.98	1.00	1.01	1.01	1.00	1.01	**1.00**	**1.00**	0.99	1.00	1.00	0.98	0.97	0.91	0.80	0.68	0.62
9	0.69	0.80	0.91	0.97	0.97	0.99	0.99	0.99	1.00	**1.00**	**1.00**	0.98	0.98	0.97	0.97	0.95	0.89	0.78	0.67	0.61
10	0.69	0.80	0.90	0.96	0.99	0.99	0.99	0.99	0.99	0.99	0.98	0.99	0.99	0.98	0.98	0.95	0.89	0.77	0.67	0.61
11	0.67	0.76	0.85	0.90	0.95	0.96	0.97	0.96	0.97	0.96	0.97	0.97	0.98	0.98	0.96	0.93	0.88	0.75	0.65	0.59
12	0.66	0.71	0.77	0.82	0.86	0.89	0.92	0.93	0.94	0.94	0.95	0.97	0.98	0.97	0.96	0.95	0.87	0.75	0.65	0.58
13	0.65	0.67	0.70	0.73	0.75	0.78	0.80	0.83	0.85	0.87	0.89	0.92	0.93	0.94	0.94	0.94	0.85	0.74	0.65	0.57
14	0.62	0.63	0.64	0.65	0.67	0.68	0.69	0.70	0.72	0.74	0.77	0.79	0.81	0.83	0.84	0.83	0.79	0.69	0.62	0.55
15	0.63	0.63	0.64	0.64	0.64	0.66	0.66	0.66	0.67	0.69	0.70	0.71	0.73	0.74	0.75	0.75	0.72	0.67	0.62	0.52
16	0.63	0.62	0.62	0.63	0.63	0.63	0.64	0.64	0.64	0.65	0.65	0.66	0.67	0.67	0.68	0.68	0.66	0.64	0.61	0.48
17	0.63	0.63	0.62	0.62	0.63	0.63	0.63	0.63	0.63	0.64	0.64	0.64	0.64	0.64	0.65	0.65	0.63	0.61	0.60	0.41

Fig. 9. (a) Dose distribution of the square dermatological applicator Amersham/SIQ18; (b) Dose distribution of the rectangular dermatological applicator Amersham/SIQ21.

Declaration of competing interest

The authors declare that they have no known competing financial interests or personal relationships that could have appeared to influence the work reported in this paper.

Acknowledgements

This work was supported by the Brazilian funding agencies FAPESP [2018/05982–0] and CNPq [140032/2020–7 and 305142/2021–6].

Data availability

Data will be made available on request.

References

Agostinelli, S., Allison, J., Amako, K., Apostolakis, J., Araujo, H., Arce, P., Asai, M., Axen, D., Banerjee, S., Barrand, G., Behner, F., Bellagamba, L., Boudreau, J., Broglia, L., Brunengo, A., Burkhardt, H., Chauvie, S., Chuma, J., Chytracek, R., Cooperman, G., Zschiesche, D., 2003. GEANT4—a simulation toolkit. Nucl. Instrum. Methods Phys. Res. Sect. A Accel. Spectrom. Detect. Assoc. Equip. 506 (3), 250–303. https://doi.org/10.1016/S0168-9002(03)01368-8.

Arce, P., Lagares, J.I., Harkness, L., Pérez-Astudillo, D., Cañadas, M., Rato, P., de Prado, M., Abreu, Y., de Lorenzo, G., Kolstein, M., Díaz, A., 2014. Gamos: a framework to do Geant4 simulations in different physics fields with a user-friendly interface. Nucl. Instrum. Methods Phys. Res. Sect. A Accel. Spectrom. Detect. Assoc. Equip. 735, 304–313. https://doi.org/10.1016/j.nima.2013.09.036.

Bevington, P.R., Robinson, D.K., 2003. Uncertainties in measurements. Data Reduction and Error Analysis for the Physical Sciences. California.

BIPM, IEC, IFCC, ILAC, ISO, IUPAC, IUPAP, OIML, 2008. Evaluation of measurement data—guide to the expression of uncertainty in measurement, JCGM 100: 2008 GUM 1995 with minor corrections. Joint Committee for Guides in Metrology 98.

CNEN, National Commission on Nuclear Energy, 2014. Basic guidelines for radiological protection. Available: http://appasp.cnen.gov.br/seguranca/normas/pdf/Nrm301.pdf. (Accessed 20 June 2023).

Cross, W.G., Hokkanen, J., Järvinen, H., Mourtada, F., Sipilä, P., Soares, C.G., Vynckier, S., 2001. Calculation of beta-ray dose distributions from ophthalmic applicators and comparison with measurements in a model eye. Med. Phys. 28 (7), 1385–1396. https://doi.org/10.1118/1.1376442.

Cross, W.G., Soares, C.G., Vynckier, S., Weaver, K., 2004. Dosimetry of beta rays and low-energy photons for brachytherapy with sealed sources, Bethesda. ICRU (Int. Comm. Radiat. Units Meas.) Rep. 72.

Dias, S.K., Caldas, L.V.E., 1998. Development of an extrapolation chamber for the calibration of beta-ray applicators. IEEE Trans. Nucl. Sci. 45 (3), 1666–1669.

Friedell, H.L., Thomas, C.I., Krohmer, J.S., 1950. Beta-ray application to the eye: with the description of an applicator utilizing 90Sr and its clinical use. Am. J. Ophthalmol. 33 (4), 525–535. https://doi.org/10.1016/0002-9394(50)90445-4.

Furetta, C., 2008. Questions and Answers on Thermoluminescence (TL) and Optically Stimulated Luminescence (OSL). World Scientific Publishing Co. Pte. Ltd., Singapore.

Furetta, C., 2010. Handbook of Thermoluminescence. World Scientific Publishing Co. Pte. Ltd., Singapore.

GAFChromic™ EBT3 film specifications. www.gafchromic.com, 2018–. (Accessed 10 July 2024).

Horowitz, Y.S., 2014. Thermoluminescence dosimetry: state-of-the-art and frontiers of future research. Radiat. Meas. 71, 2–7.

ISO (International Organization for Standardization), 2009. Clinical Dosimetry - Beta Radiation Sources for Brachytherapy. ISO 21439:2009, Geneva.

ISO (International Organization for Standardization), 2023. Nuclear Energy - Reference Beta-Particle Radiation - Part 2: Calibration Fundamentals Related to Basic Quantities Characterizing the Radiation Field. Geneva. ISO 6980-2:2023.

Kry, S.F., Alvarez, P., Cygler, J.E., DeWerd, L.A., Howell, R.M., Meeks, S., Mihailidis, D., 2020. Aapm TG 191: clinical use of luminescent dosimeters: TLDs and OSLDs. Med. Phys. 47 (2), e19–e51.

McKeever, S.W.S., Moscovitch, M., Townsend, P.D., 1995. Thermoluminescence Dosimetry Materials: Properties and Uses. Nuclear Technology Publishing, Ashford.

Mostafa, L., Rachid, K., Ahmed, S.M., 2016. Comparison between beta radiation dose distribution due to LDR and HDR ocular brachytherapy applicators using GATE Monte Carlo platform. Phys. Med. 32 (8), 1007–1018.

Niroomand-Rad, A., Chiu-Tsao, S.-T., Grams, M.P., Lewis, D.F., Soares, C.G., van Battum, L., Das, I.J., Trichter, S., Kissick, M.W., Massillon-Jl, G., Alvarez, P.E., Chan, M.F., 2020. Report of AAPM task group 235 radiochromic film dosimetry: an update to TG-55. Med. Phys. 47 (12), 5986–6025. https://doi.org/10.1002/mp.14497.

Rosa, A.A., de Sousa, C.F.P.M., Pimentel, L.C.F., Martins, H.L., Moraes, F.Y., Marta, G.N., Castilho, M.S., 2023. Radiotherapy resources in Brazil (RT2030): a comprehensive analysis and projections for 2030. Lancet Oncol. 24 (8), 903–912.

Soares, C.G., 1991. Calibration of ophthalmic applicators at NIST: a revised approach. Med. Phys. 18 (4), 787–793.

Soares, C.G., 1995. Comparison of NIST and manufacturer calibrations of ^{90}Sr+ ^{90}Y ophthalmic applicators. Med. Phys. 22 (9), 1487–1493.

Soares, C.G., 2006. New developments in radiochromic film dosimetry. Radiat. Protect. Dosim. 120, 100–106.

Soares, C.G., Trichter, S., Devic, S., 2009. Radiochromic film. In: Rogers, D.W.O., Cygler, J.E. (Eds.), Clinical Dosimetry for Radiotherapy: AAPM Summer School. Medical Physics Publishing, Madison, WI, pp. 759–813. ISBN 9781888340846), Chap. 23.

Soares, C.G., Vynckier, S., Järvinen, H., Cross, W.G., Sipilä, P., Flühs, D., Schaeken, B., Mourtada, F.A., Williams, T.T., 2001. Dosimetry of beta-ray ophthalmic applicators: comparison of different measurement methods. Med. Phys. 28 (7), 1373–1384. https://doi.org/10.1118/1.1376441.

SUS (Sistema Único de Saúde), Ministry of Health: Brasília-DF, 2022. Manual of technical bases for oncology. In: Ambulatory Information System Edition 30, 30, pp. 152–155. http://www1.inca.gov.br/inca/Arquivos/comunicacao/manual_de_bases_tecnicas_oncologia.pdf. (Accessed 10 July 2024). In Portuguese.